CH9800022

Study of second stability for ITG modes

M. Fivaz, O. Sauter, K. Appert, S. Brunner, T. M. Tran, J. Vaclavik

Centre de Recherches en Physique des Plasmas, Association Euratom-Confédération Suisse
EPFL, PPB, 1015 Lausanne, Switzerland

Abstract The second stability regime for ion-temperature-gradient (ITG) modes is studied in details with a global linear gyrokinetic Particle-In-Cell code which takes the full toroidal MHD equilibrium data. The trapped-ion and the toroidal ITG regimes are explored. We perform simultaneous ideal MHD stability computations for both kink ($n = 1$) and ballooning ($n = \infty$) modes. We use the results to find partially optimized configurations that are stable to ideal MHD modes and where the ITG modes are stable or have very low growth rates. Such configurations are expected to have very low level of ITG-induced transport.

Introduction. Unstable ITG modes are now commonly held responsible for anomalous ion heat transport in tokamaks. The ion temperature gradient provides free energy to the instability and the magnetic field gradient provides an efficient destabilizing mechanism on the outer side of the torus. These modes are stable when the ion temperature gradient is below a critical values (first stability regime). At high pressure, the plasma diamagnetism can reduce of even reverse the gradient of the equilibrium magnetic field, which then becomes favorable everywhere in the plasma; the ITG modes can then be completely stabilized [1] in what can be called a second stability regime. This effect is sometimes referred to as "Shafranov-shift stabilization".

Previous calculation [2] [3] [4] are undetailed and were done using the ballooning approximation and (except [2]) with the "$s - \alpha$" approximation to the equilibrium magnetic field, a high aspect ratio, circular shifted magnetic surface approximation. The ballooning approximation, though, breaks down at low n or low magnetic shear, and cannot describe slab-like modes that are not localized on the outer side of the torus, i.e. that do not "balloon". The "s-α" model also breaks down at realistic aspect ratio and in non-circular plasmas.

We study here in detail the conditions that lead to the second stability for ITG modes, using a global approach (no ballooning approximation) and the full MHD equilibrium data. We focus on cases where a low magnetic shear stabilizes the local, short wavelength MHD ballooning modes. We use the code GYGLES (GYrokinetic Global LinEar Solver)[5] [6], which uses a radially global approach in toroidal geometry. The simulation model is based on the linear gyrokinetic equations for the ions in which the full guiding center trajectories are kept. We assume the electrons to respond adiabatically and the equilibrium perturbation to be electrostatic and quasineutral. The gyrokinetic equations are linearized around an equilibrium local Maxwellian distribution function. The code uses a Particle-In-Cell method with finite elements defined in magnetic coordinates. The code can simulate routinely global modes of all (very short to very long) toroidal wavelengths, can treat realistic (MHD) equilibria of any

Global parameters	$R_0 = 3$ m, $a/R_0 = 1/.36$, elong. 1.6, triang. .3, vac. field $B_0(R_0) = 3$ T, $\rho \approx 4.8$ mm (deuterium)
Temperatures	$\frac{T_i}{dT_i/ds} = -\frac{1}{2}\kappa_T \left(1 + \cos\left[\frac{\pi}{2}\frac{s-s_0}{\Delta s}\right]\right)$ for $\lvert s - s_0\rvert < 2\Delta s$, 0 elsewhere $\kappa_T = \frac{1}{\Delta s}\log(T_{mul})$, $s_0 = .6$, $\Delta s = 0.1$, $T_i(s_0) = 10$ Kev, $T_e = T_i$
Density profile	$n_i(s) = n_0(1 - s^2)^4$
Norm. current density	$\hat{I}^*(s) = j_0(1 - s^2) + j_a \exp\left[-\frac{(s-s_0)^2}{\Delta s_j^2}\right]$ $j_a = T_{mul} * (.14 * j_0 + .24)$, $\Delta s_j = 0.15$
Scan parameters	$j_0 \in [.8, 100]$, $T_{mul} \in [1.1, 1.8]$
Parameters at $s = s_0$	$R_0/L_T \equiv \kappa_T R_0/a$, $R_0/L_n = 2.8$, $q = 1.5$, shear $\hat{s} \approx 0.2$

Table 1: *Specification of the equilibria studied.*

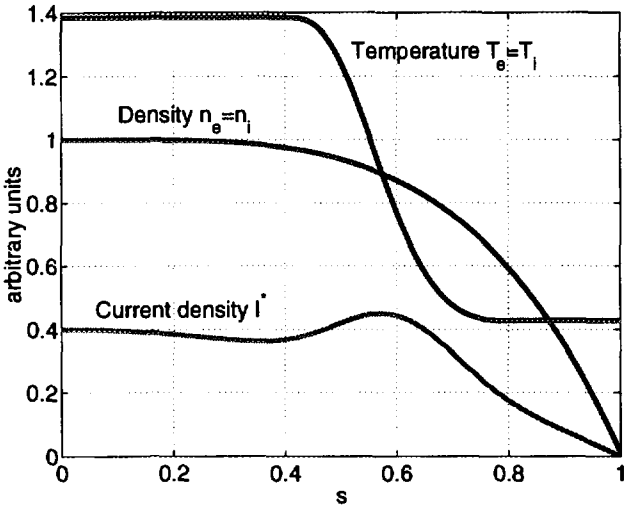

Figure 1: *Profiles from table (1).*

size and runs on a massively parallel computer.
The inclusion of electromagnetic perturbations can affect (usually stabilize further) ITG modes at high β [7] [4] [8] [9]. This effect is not included here; we focus rather on the stabilizing effect of the modification of the equilibrium at high β using realistic (MHD) equilibrium magnetic structure.

Parametric study. We introduce a radial variable $s = \sqrt{\Psi/\Psi_a}$, where Ψ is the equilibrium poloidal magnetic flux and Ψ_a its value at the plasma boundary, the plasma major and minor radii R_0 and a and the normalized temperature gradient $\frac{R_0}{L_T} \equiv \frac{R_0}{a}\frac{\partial T/\partial s}{T}$. Locally on the outer plasma mid-plane, one can derive from the MHD equilibrium condition a criterion for magnetic gradient reversal:

$$\alpha \equiv -\mu_0 \frac{R}{B_t^2}\frac{\partial p}{\partial R} > 1$$

The reversal parameter α is such that $\alpha = 0$ at low pressure and $\alpha > 1$ when the magnetic field gradient is reversed on the outer mid-plane. It is therefore a local parameter characterizing the magnetic field gradient at the most unfavorable point. It differs by a factor q^2 from the usual α parameter from "$s - \alpha$" equilibria and that is important in MHD ballooning computations. The table (1) defines a set of JET-size equilibria where the profile of R_0/L_T is inspired by a high-confinement JT60-U discharge [10] and peaks at a given magnetic surface at $s = s_0$, thus confining the unstable modes around that surface. In what follows, R_0/L_T and α refer to their values at $s = s_0$. Both α and R_0/L_T can be chosen by varying the parameters j_0 and T_{mul}. In the region where the modes lie, the safety factor does not depend on R_0/L_T and α. The magnetic shear $\hat{s}$ is low, $0 < \hat{s} < 0.2$, where the modes lie. This has the effect that all these equilibria are stable to MHD ballooning modes; in particular, equilibria with high pressure gradients lie in the second stability zone [12].
We use this set to do a generic study of ITG stability as a function of R_0/L_T and α at fixed safety factor profile, in both the regimes of toroidal ITG (high toroidal mode number n, mode frequency $\equiv \omega > \omega_b \equiv$ trapped-ion bounce frequency) and the trapped-ion regimes (low n, $\omega < \omega_b$).
The profiles of the surface-averaged current $I^*(s)$ and of the pressure $p(s) = n_i(s)\,(T_e(s) + T_i(s))$ are first used to solve the Grad-Shafranov equation with the code CHEASE [11], yielding the magnetic field structure that is then used by GYGLES to compute ITG stability.

Results. Figure (2) shows the contours of the growth rates obtained for $n = 12$ and $n = 48$ in the (α,R_0/L_T) plane. The frequency of these modes increases with R_0/L_T and with n, while

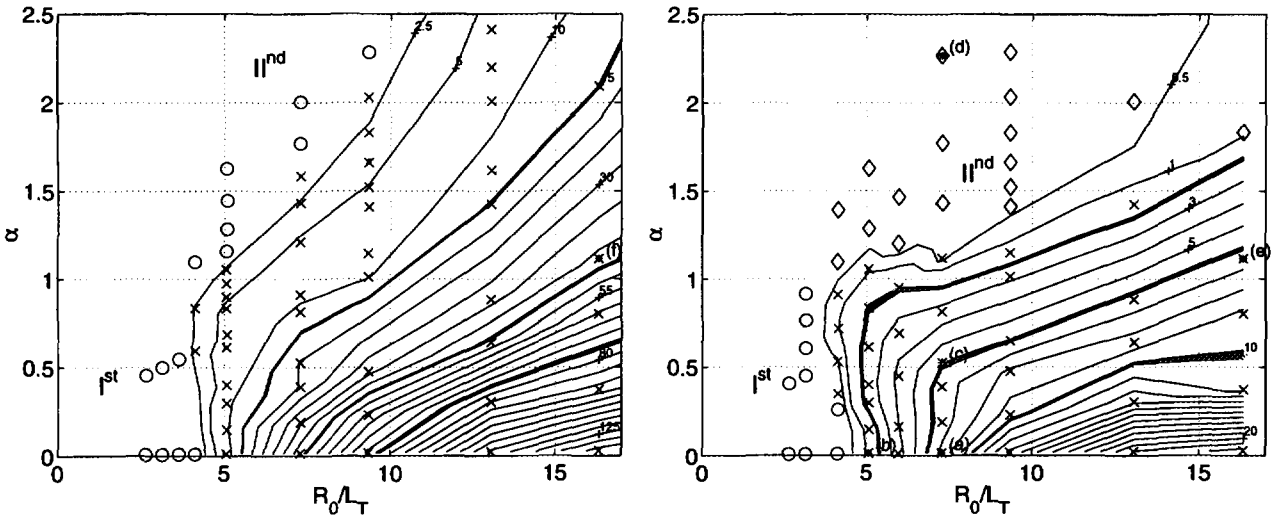

Figure 2: *Contours of the growth rate (in kHz). Left: n=48, Toroidal ITG regime. Right: n=12, Trapped-ion mode regime. The crosses (o), circles (x) and diamond (◇) represent respectively equilibria that were found stable, unstable to toroidal modes, and very weakly unstable to slab-like modes.*

the ion bounce frequency ω_b is fixed. As a results, the $n = 12$ modes are in the trapped-ion regime with $\omega < \omega_b$, except at high R_0/L_T, where they have a small toroidal ITG character. Conversely, the $n = 48$ modes are in the toroidal ITG regime, except at very low values of R_0/L_T.

We call "first stability zone" the stable zone, marked "Ist" on Fig. 2, that lies below a critical temperature gradient. Above this gradient, the mode is stabilized for increasing α as ∇B decreases and is reversed for $\alpha \geq 1$, leading to the "second stability zone" for ITG modes, marked "IInd" on the same figure. In the toroidal ITG regime, these equilibria are fully stable, while in the trapped-ion regime, a weakly unstable slab-like ITG mode remains. The second stability regime is therefore strictly stable to toroidicity-related modes only (at least at low shear), but the slab-like modes are not expected to cause much anomalous transport, as they are radially narrow and very weakly unstable. The structure of the eigenmodes marked (a) (a trapped-ion mode) and (d) (a slab-like ITG mode) on Fig. (2), are shown in Fig. (3). The contours of growth rates corresponding to mixing-length estimates of the heat diffusivity $\chi_\perp = 1$, 3 and 5 m^2/s are shown in bold in Fig. (2). While these values should not be taken as more than rough estimates, they show that the scan covers most of the experimentally relevant range of $0.1 - 10$ m^2/s.

MHD stability calculations. The CHEASE code was used to compute the stability of MHD ballooning modes. All the equilibria presented here are stable to these modes at the surface $s = s_0$; this was achieved by lowering the magnetic shear to a $0 < \hat{s} < 0.2$, so pushing the equilibria with high values of α into the second stability regime for ballooning modes. Kinetic effects on these modes were not considered [4]. This demonstrates the existence of a simultaneous second stability regime for ITG modes and for MHD ballooning modes. The code ERATO [13] was used to compute the stability to kink modes. The points (a), (c) and (e) on Fig. (2), the latter at $\alpha = 1.1$, are stable to the global n=1 kink mode; stability at values of α that are roughly 50% higher is obtained if an ideal wall is added at $r_{wall}/a = 1.2$, assuming sufficient toroidal rotation and wall stabilization effect. In particular, the equilibrium corresponding to the point at $R_0/L_T = 16.3$ and $\alpha = 1.8$ is MHD-stable with an ideal wall and is only weakly unstable to ITG modes; it is the most interesting global case in our scan. The corresponding profiles are those of Fig. (1).

Conclusions. We studied the simultaneous access to second stability for ITG modes and for

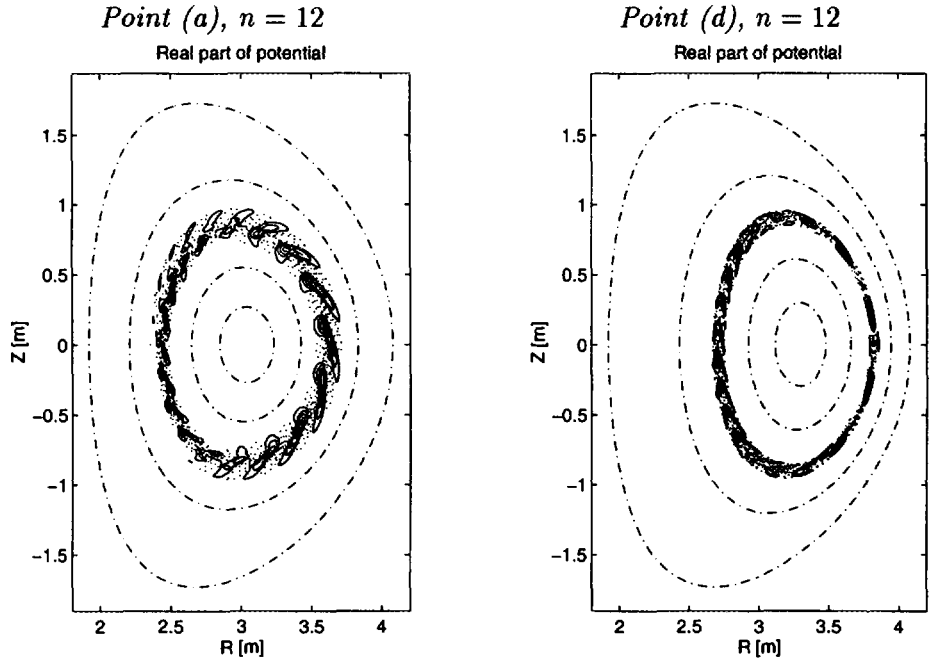

Figure 3: *Eigenmodes corresponding to the points (a) and (d) shown in Fig. (2).*

ballooning modes. The MHD ballooning modes are stabilized by low shear on the surface of interest in all the configurations presented. The stabilization of ITG modes is well described by the local magnetic field gradient reversal parameter α, and any ITG-induced transport should be strongly reduced for $\alpha \approx 1$.
Global kink modes are stable without ideal wall up to relatively high values of α, $\alpha = 1.1$ for $R_0/L_T = 16.3$. When a ideal wall at r_{wall}/a=1.2 is included, one obtains stability at $\alpha = 1.8$ for the same temperature gradient. This equilibrium has therefore good MHD properties and should have sustainable ITG transport ($\chi_\perp \approx 1$ m^2/s, Fig. (2)) while its temperature gradient is three times higher than the critical gradient at low β. By optimizing the plasma shape and profiles, we expect to find in the near future improved optimized high-performance configurations that are stable to all ideal MHD modes and stable or weakly unstable only to global ITG modes.
We finally note that some experimental discharges seem to have accessed $\alpha \approx 1$ [6].
This research work was supported in part by the Swiss National Science Foundation and the Cray-EPFL PATP project. The computations were done on the Cray-T3D parallel supercomputer of the EPFL-PATP.

References

[1] M. Fivaz *et al.*, Phys. Rev. Lett. **78**, 3471 (1997).
[2] G. Rewoldt, W. M. Tang, and M. S. Chance, Phys. Fluids **25**, 480 (1982).
[3] X. Q. Xu and N. M. Rosenbluth, Phys. Fluids B **3**, 627 (1991).
[4] M. Yamagiwa, A. Hirose, and M. Elia, Plasma Phys. Control. Fusion **39**, 531 (1997).
[5] M. Fivaz *et al.*, submitted to Computer Physics Communications **0**, 0 (1997).
[6] M. Fivaz, PhD thesis No. 1692, Ecole polytechnique Fédérale de Lausanne, Switzerland, 1997.
[7] J. Y. Kim, W. Horton, and J. Q. Dong, Phys. Fluids B **5**, 4030 (1993).
[8] R. R. Domingez and R. W. Moore, Nucl. Fusion **26**, 85 (1986).
[9] A. Jarmen, P. Anderson, and J. Weiland, Nucl. Fusion **27**, 941 (1987).
[10] Y. Neyatani and the JT60-Team, Plas. Phys. Control. Fusion **38**, A181 (1996).
[11] H. Lütjens, A. Bondeson, and O. Sauter, Comput. Phys. Commun. **97**, 219 (1996).
[12] D. Lortz and J. Nührenberg, Phys. Lett. **68A**, 49 (1978).
[13] R. Gruber *et al.*, Comput. Phys. Commun. **21**, 323 (1981).